[第19回日本レーザー医学会大会報告]

〈招待講演〉

Optical Coherence Tomography: A New Technology for Biomedical Imaging

James G. Fujimoto[1], Stephen Boppart[1,2], Costas Pitris[1,2], and Mark Brezinski[3]

[1]Department of Electrical Engineering and Computer Science
and Research Laboratory of Electronics
Massachusetts Institute of Technology
Cambridge, MA 02139, USA
Tel: 617 253-8528 Fax: 617 253-9611

[2]Health Sciences and Technology Division
Massachusetts Institute of Technology
and Harvard Medical School
Boston, MA 02115

[3]Department of Medicine and Cardiac Unit
Harvard Medical School
and Massachusetts General Hospital
Boston, MA 02114

Abstract

Optical coherence tomography (OCT) is a new technology for performing high resolution cross sectional imaging. OCT is analogous to ultrasound imaging, except that it uses light instead of sound. OCT can provide cross sectional images of tissue structure on the micron scale in situ and in real time. Using OCT in combination with catheters and endoscopes enables high resolution intraluminal imaging of organs. OCT functions as a type of optical biopsy and is a powerful imaging technology for medical diagnostics because unlike conventional histopathology which requires removal of a tissue specimen and processing for microscopic examination, OCT can provide images of tissue in situ and in real time. OCT can be used where standard excisional biopsy is hazardous or impossible, to reduce sampling errors associated with excisional biopsy, and to guide interventional procedures. In this paper, we review OCT technology and describe its potential medical applications.

Introduction

Optical coherence tomography (OCT) is a new optical imaging technique that performs high resolution, cross-sectional tomographic imaging of the internal microstructure in biological systems [1]. OCT is analogous to ultrasound B mode imaging except that it uses light instead of sound. Image resolutions of 2-15 um can be achieved, over one order of magnitude higher than conventional clinical ultrasound. OCT performs imaging by measuring the echo time delay and intensity of backscattered light from internal microstructure in the tissue. OCT images are a two-dimensional data set which represent the optical backscattering in a cross sectional plane through the tissue.

modality [2-6]. Working in collaboration with the New England Eye Center, several thousand patients have been examined to date. The technology was transferred to industry and introduced commercially for ophthalmic diagnostics in 1996 (Humphrey Systems, Dublin, CA).

More recently, advances in OCT technology have made it possible to image nontransparent tissues, thus enabling OCT to be applied in a wide range of medical specialties [7-9]. Imaging depth is limited by optical attenuation from tissue scattering and absorption. However, imaging up to 2-3 mm deep can be achieved in most tissues. This is the same scale as that typically imaged by conventional biopsy and histology. Although imaging depths are not as deep as with ultrasound, the resolution of OCT is more than 10 times finer than standard clinical ultrasound. OCT has been applied in vitro to image arterial pathology and can differentiate plaque morphologies [8,10]. Imaging studies have also been performed in vitro to investigate applications in dermatology, gastroenterology, urology, gynocology, surgery, neurosurgery, and rheumatology [11-20]. OCT has also been applied in vivo to image developing biological specimens (African frog, leopard frog, and zebrafish tadpoles and embryos) [21-23]. For applications in developmental biology, OCT allows repeated imaging of developing morphology without the need to sacrifice specimens.

Numerous developments in OCT technology have also been made. OCT has been

interfaced with catheters, endoscopes, and laparoscopes [24-26]. High speed and high resolution OCT imaging has been demonstrated [27-29]. Cellular level OCT imaging has recently been demonstrated in developmental biology [30]. Catheter and endoscope OCT imaging of the gastrointestinal and pulmonary tracts as well as arterial imaging has been demonstrated in vivo in an animal model [31]. Preliminary endoscopic OCT studies in human subjects have been reported [32]. Studies in patients are currently being performed by our group as well as other groups.

In general, there are three types of clinical scenarios where we believe that OCT could have important applications: 1. Where conventional excisional biopsy is hazardous or impossible, 2. Where conventional biopsy has an unacceptably high false negative rate because of sampling errors, and 3. For guidance of surgical interventional procedures. In this manuscript, we review the fundamental concepts of OCT imaging, technology, and discuss potential applications to biomedical research and clinical medicine.

Principles of operation and technology

OCT is analogous to ultrasound imaging but uses light instead of sound. Cross sectional images are generated by measuring the echo time delay and intensity of light which is reflected or backscattered from internal microstructure in tissue. Because the velocity of light is extremely high, its echo time delay cannot be measured directly by electronics as in ultrasound. Instead, it is necessary to use correlation or interferometry techniques. One method for measuring the echo time delay of light is to use low coherence interferometry. Low coherence interferometry was first developed for measuring reflections in fiber optics and optoelectronic devices [33,34]. The first applications of low coherence interferometry in biomedicine were in ophthalmology to perform precision measurements of axial eye length and corneal thickness [35-37].

Low coherence interferometry measures the echo time delay and intensity of backscattered light by comparing it to light that has traveled a known reference path length and

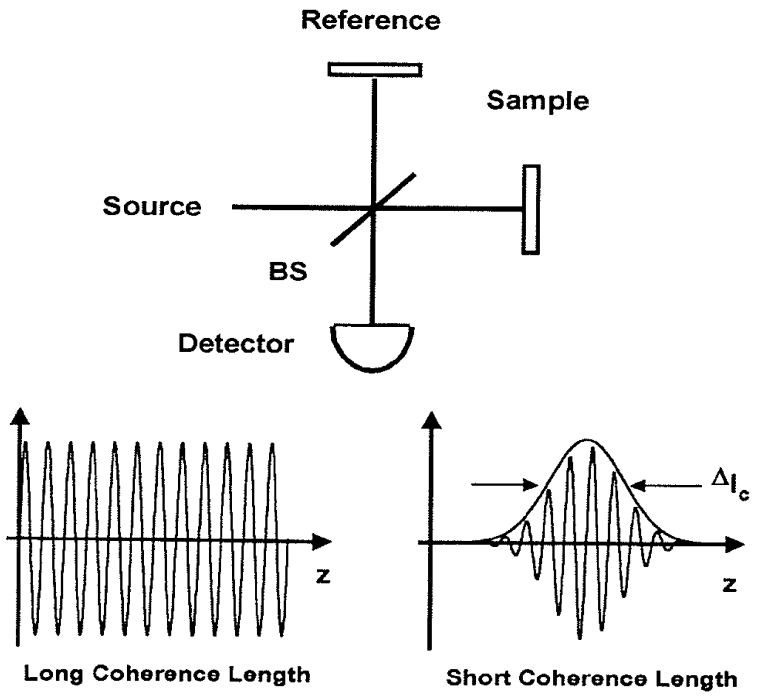

Fig. 1. OCT measures the echo time delay of reflected light by using low coherence interferometry. The system is based on a Michelson type interferometer. Reflections or backscattering from the object being imaging are correlated with light which travels a reference path.

time delay. Measurements are performed using a Michelson type interferometer (Figure 1). Light from a source is directed onto a beam splitter and one of the beams is incident onto the sample to be imaged, while the second beam travels a reference path with a variable path length and time delay. The backscattered light from the sample is interfered with reflected light from the reference arm and detected with a photodetector at the output of the interferometer. If the light source is coherent, then interference fringes will be observed as the relative path lengths are varied. However if low coherence or short pulse light is used, then interference of the light reflected from the sample and reference path can occur only when the two path lengths match to within the coherence length of the light. The echo time delay and intensity of backscattered light from sites within the sample can be measured by detecting and demodulating the interference output of the interferometer while scanning the reference path length.

Figure 2 is a schematic illustrating how OCT performs cross sectional imaging. The

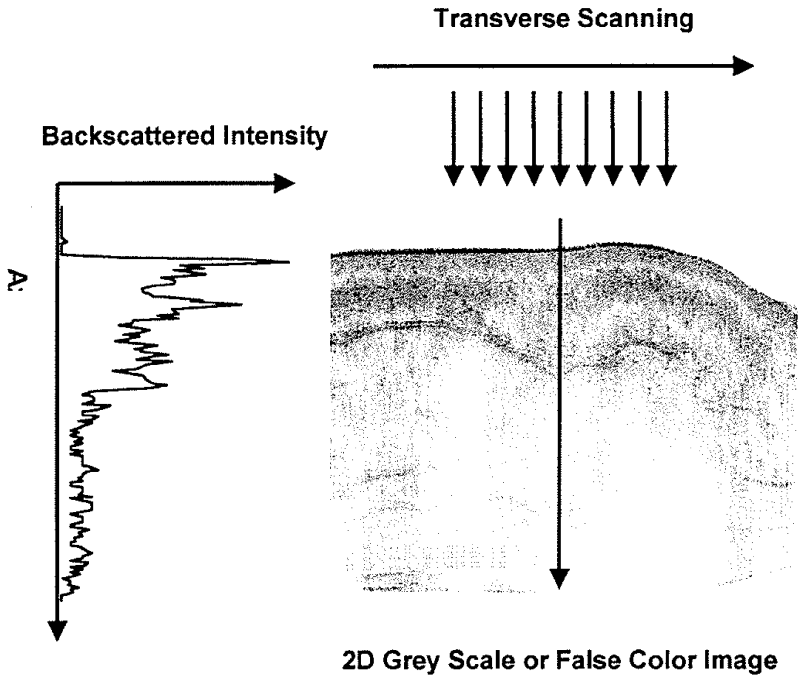

Fig. 2. Cross sectional images are constructed by performing measurements of the echo time delay of light at different transverse positions. The result is a two dimensional data set which represents the backscattering in a cross sectional plane of the tissue.

optical beam is focussed into the sample being imaged and the echo time delay and intensity of the backscatered light is measured to yield an axial backscattering profile. The incident beam is then scanned in the transverse direction and the axial backscattering profile is measured at several transverse positions to yield a two dimensional data set. This data set represents the optical backscattering through a cross section of the tissue. The data is displayed as a logarithmic gray scale or false color image.

In contrast to conventional microscopy, the mechanisms which govern the axial and transverse image resolution in OCT are decoupled. The axial resolution in OCT imaging is determined by the coherence length of the light source so high resolution can be achieved independent of the beam focussing conditions. The interference signal detected at the output of the interferometer is the electric-field autocorrelation of the light source. The coherence length is the spatial width of this field autocorrelation. In addition, the envelope of the field autocorrelation is equivalent to the Fourier transform of the power spectrum. Thus, the width of

the autocorrelation function, or the axial resolution, is inversely proportional to the width of the power spectrum. For a source with a Gaussian spectral distribution, the axial resolution Δz is:

$$\Delta z = (2\ln 2/\pi)(\lambda^2/\Delta\lambda)$$

where Δz and $\Delta\lambda$ are the full-widths-at-half-maximum of the autocorrelation function and power spectrum respectively and λ is the source center wavelength. The axial resolution is inversely proportional to the bandwidth of the light source and thus high resolution may be achieved by using broad bandwidth optical sources.

The transverse resolution achieved with an OCT imaging system is determined by the focused spot size as in conventional microscopy. The transverse resolution is:

$$\Delta x = (4\lambda/\pi)(f/d)$$

where d is the spot size on the objective lens and f is its focal length. High transverse resolution can be obtained by using a large numerical aperture and focusing the beam to a small spot size. In addition, the transverse resolution is also related to the depth of focus or the confocal parameter b which is $2z_R$, two times the Raleigh range:

$$2z_R = \pi\Delta x^2/2\lambda$$

Increasing the transverse resolution (smaller Δx) produces a decrease in the depth of focus, similar to conventional microscopy.

Finally, the signal to noise of detection can be calculated using standard techniques from optical communications theory and is given by:

$$SNR = 10\ \mathrm{Log}(\eta P/h\nu\ NEB)$$

where P is the detected power, NEB is the noise equivalent bandwidth of the detection, η is the detector quantum efficiency, and $h\nu$ is the photon energy. The signal to noise ratio scales as the reflected or backscattered power divided by the noise equivalent bandwidth of the detection. This means that high image acquisition speeds or higher image resolutions require higher optical powers for a given signal to noise ratio.

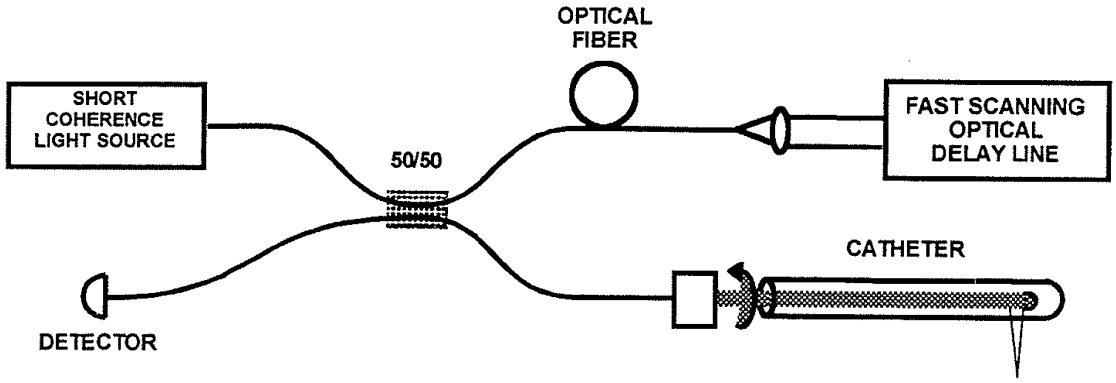

Fig. 3. Schematic of OCT instrument based on a fiber optic implementation of a Michaelson interferometer. One arm of the interferometer is interfaced to the measurement instrument and the other arm has a scanning delay line. The system shown is configured for high speed catheter-endoscope based imaging.

One of the advantages of OCT is that it can be implemented using compact fiber optic components and integrated with a wide range of medical instruments. Figure 3 shows a schematic of an OCT system using fiber optic Michelson type interferometer. A low coherence light source is coupled into the interferometer and the interference at the output is detected with a photodiode. One arm of the interferometer emits a beam which is directed and scanned on the sample which is being imaged, while the other arm of the interferometer is a reference arm with a scanning delay line.

For research applications, short pulse lasers are used as light sources for OCT imaging because they have extremely short coherence lengths and high output powers, enabling high resolution, high speed imaging. Many of our studies were performed using a short pulse Cr^{4+}:Forsterite laser. This laser produces output powers of 100 mW generating ultrashort pulses at wavelengths near 1300 nm and can produce bandwidths sufficient to achieve an axial resolution of 5-10 μm [29]. Using incident powers in the 1-10 mW range and typical image acquisition speeds of several frames per second, signal to noise ratios of 100 dB are achieved. In other studies, a short pulse Ti:Al_2O_3 laser operating near 800 nm has been used to achieve axial resolutions of 4 um [28]. Most recently, with the development of even short pulse laser sources, we have demonstrated axial resolutions of less than 2 um [38]. For clinical applications,

compact superluminescent diodes or semiconductor based light sources can be used. Commercially available (AFC Technologies Inc., Hull, Quebec, Canada) sources operating at 1.3 um can achieve axial resolutions of ~ 15 um with output powers of 10 - 15 mW, sufficient for real time OCT imaging.

High speed OCT imaging also requires technology for high speed optical delay scanning of the reference path length. Many of our studies were performed using a high speed scanning optical delay line based on a diffraction grating phase control device [39]. This device is similar to pulse shaping devices that used in femtosecond optics [40,41]. The grating phase control scanner is attractive because it achieves extremely high scan speeds and also permits the phase and group velocity of the scanning to be independently controlled. Images of 250 to 500 transverse pixels can be produced at 4-8 frames per second [31]. This technology can be scaled to perform imaging at even higher image acquisition speeds.

Biomedical Applications

Ophthalmic Imaging

OCT was initially applied for imaging of the eye [2-6]. To date, OCT has had the largest

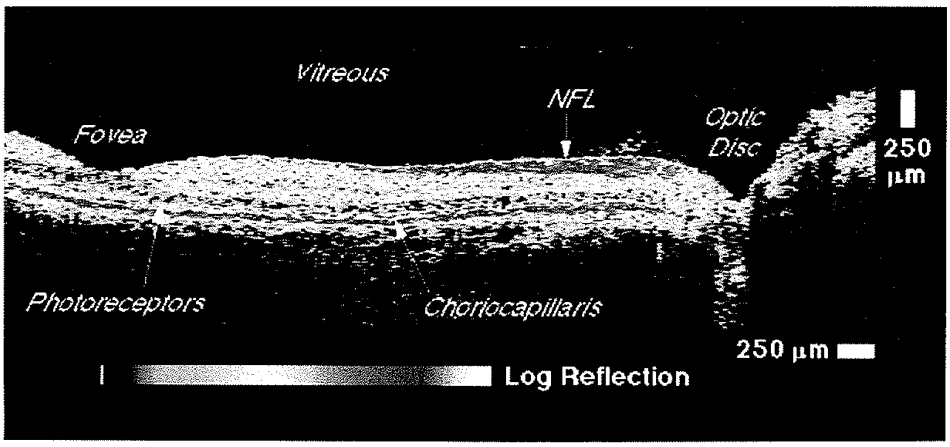

Fig. 4 OCT image of the human retina papillary-macular axis illustrating the ability to discriminate structural morphology in vivo. The highly backscattering retinal nerve fiber layer (NFL) and choriocapillaris appear red. The optic disk as well as several of the retinal layers are observed. From reference [4].

clinical impact in ophthalmology. Figure 4 shows an example of an OCT image of the normal retina of a human subject [4]. This image is 250 transverse pixels wide using a wavelength of 800 nm with a 10 um resolution. The OCT image provides a cross sectional view of the retina with unprecedented high resolution and allows detailed structures to be differentiated. Although the retina is almost transparent and has extremely low optical backscattering, the high sensitivity of OCT imaging allows extremely weak backscattering features such as the vitreal-retinal junction to be visualized. The retinal pigment epithelium and choroid, which is highly vascular, are visible as highly scattering structures in the OCT image. The retinal nerve fiber layer is visible as a scattering layer originating from the optic disk and becoming thinner approaching the fovea. The total retinal thickness as well as the retinal nerve fiber layer thickness can be measured. Since these images have a resolution of 10 um, there can be residual motion of the patient's eye on the 1-2 second time scale necessary for the measurement. However, since OCT measures absolute position, image processing algorithms can be used to measure the axial motion of the eye and correct for motion artifacts [2].

Clinical studies have been performed to investigate the feasibility of using OCT for the diagnosis an monitoring of retinal diseases such as glaucoma, macular edema, macular hole, central serous chorioretinopathy, age related macular degeneration, epiretinal membranes, optic disc pits, and choroidal tumors [42-53]. In addition, the ability of OCT to perform real time imaging has also been used to study dynamic responses of the retina including retinal laser injury [54,55]. Images can be analyzed quantitatively and processed using intelligent algorithms to extract features such as retinal or retinal nerve fiber layer thickness [43-46]. Mapping and display techniques have been developed to represent the tomographic data in alternate forms, such as thickness maps, in order to aid interpretation. OCT is especially promising for the diagnosis and monitoring of diseases such as glaucoma or macular edema associated with diabetic retinopathy because it can provide quantitative information retinal pathology which is a measure of disease progression. OCT has the potential to detect and diagnose early stages of

disease before physical symptoms and irreversible loss of vision occurs.

Optical Coherence Tomography and Optical Biopsy

With recent research advances, OCT imaging of optically scattering, nontransparent tissues is possible, thus enabling a wide variety of applications in internal medicine and internal body imaging [7-9]. One of the most important advances for imaging in optically scattering tissues was the use of longer wavelengths where optical scattering is reduced [56,57]. By performing OCT imaging at 1.3 um wavelengths, image penetration depth of 2 to 3 millimeters can be achieved in most tissues. This imaging depth is comparable to the depth over which many biopsies are performed. In addition, many diagnostically important changes of tissue morphology occur at the epithelial surfaces of organ lumens. The capability to perform in situ and real time imaging could be important in a variety of clinical scenarios including: 1. To perform imaging of tissue microstructure in situations where conventional excisional biopsy would be hazardous or impossible, 2. To reduce false negative rates due to sampling errors of conventional biopsy, and 3. To guide surgical or microsurgical intervention.

Imaging where excisional biopsy is hazardous or impossible

One class of applications where OCT could be especially powerful is where conventional excisional biopsy is hazardous or impossible. In ophthalmology, retinal biopsy cannot be performed and OCT can provide high resolution images of pathology that cannot be obtained using any other technique [2-6]. OCT imaging can be performed repeatedly for screening or to track disease progression. Another scenario where biopsy is not possible is imaging of atherosclerotic plaque morphology in the coronary arteries [8-10]. Recent research has demonstrated that most myocardial infarctions result from the rupture of small to moderately sized cholesterol-laden coronary artery plaques followed by thrombosis and vessel occlusion [58-62]. The plaques at highest risk for rupture are those which have a structurally weak fibrous cap.

These plaque morphologies are difficult to detect by conventional radiologic techniques and their microstructural features cannot be determined. Identifying high risk unstable plaques and patients at risk for myocardial infarction is important because of the high percentage of occlusions which result in sudden death [63]. OCT could be powerful for diagnostic intravascular imaging in both risk stratification as well as guidance of interventional procedures such as atherectomy.

In vitro imaging studies of arterial lesions were performed to investigate the correlation of OCT and histology [8,10]. Figure 5 shows an example of an unstable plaque morphology from a human abdominal aorta specimen and corresponding histology. Specimens were obtained after autopsy and were imaged by OCT using a microscope delivery system prior to fixation. OCT imaging was performed at 1300 nm wavelength using a superluminescent diode light source with

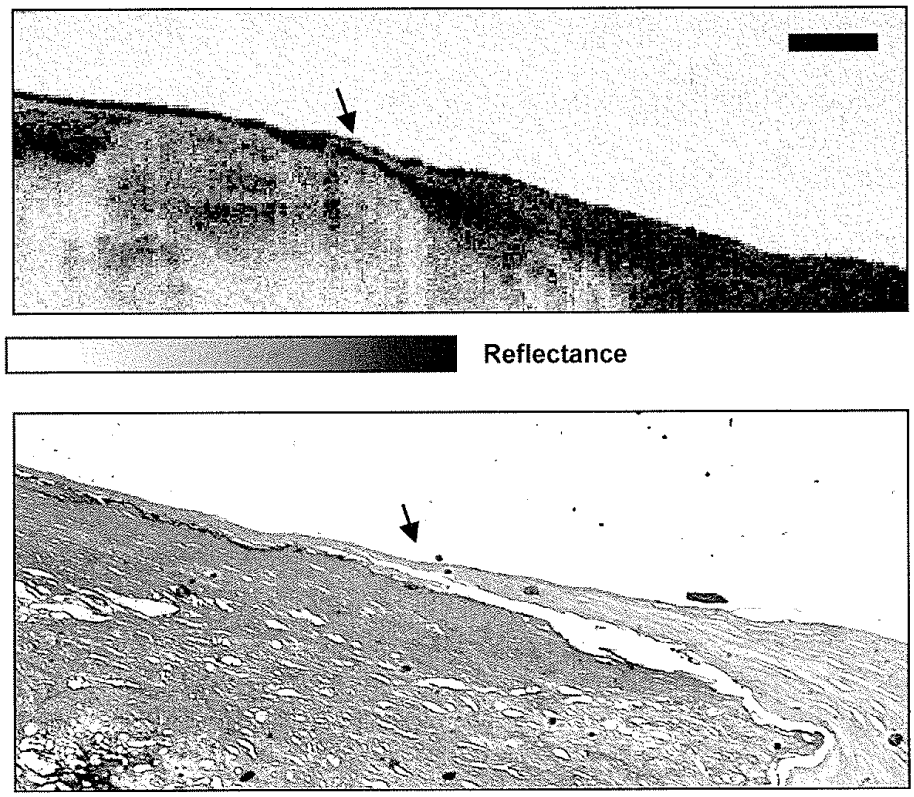

Fig. 5 In vitro OCT image of atherosclerotic plaque and corresponding histology. The plaque is heavily calcified with a low lipid content. A think intimal layer covers the plaque. The high resolution of OCT can resolve small structures such as the thin intimal layer which are associated with unstable plaques. The bar is 500 um. From reference [8].

an axial resolution of ~16 um. The OCT image and histology show a small intimal layer covering a large atherosclerotic plaque which is heavily calcified and has a relatively low lipid content. The optical scattering properties of lipid, adiopse tissue, and calcified plaque are different and provide contrast between different structures and plaque morphologies.

The rupture of unstable atherosclerotic plaques in coronary arteries is now believed to be the most common cause of acute myocardial infarction [58-62]. Conventional clinical imaging modalities such as angiography, ultrasound, or MRI do not have sufficient resolution to identify these lesions or to guide the removal of plaque catheter via based atherectomy procedures. High frequency (20-30 MHz) intravascular ultrasound or IVUS can be used to determine the extent of arterial stenosis as well as guide intervention procedures such as stent deployment [64,65]. However, the resolution of IVUS is limited to approximately 100 um and thus it is difficult to identify high risk plaque morphologies [66]. Studies have been performed which compare IVUS and OCT imaging in vitro and demonstrate the ability of OCT to identify clinically relevant pathology [10]. In vivo OCT arterial imaging has also been performed in New Zealand White rabbits using a catheter based delivery system [67]. Optical scattering from blood limits OCT imaging penetration depths so that saline flushing at low rates was required for imaging. These effects depend on vessel diameter as well as other factors and additional investigation is required.

Detecting Early Neoplastic Changes

Another important class of OCT imaging applications is in situations where conventional excisional biopsy has unacceptably high false negative rates due to sampling errors. This situation occurs in the screening and detection early neoplastic changes. OCT can resolve changes in architectural morphology which are associated with many early neoplastic changes. In vitro studies have been performed to investigate OCT imaging in the gastrointestinal, urinary, respiratory, and female reproductive tracts [11-14,19,68,69]. Preliminary in vivo studies in human subjects have also been performed [32,70]. Figure 6 shows an example of an OCT image

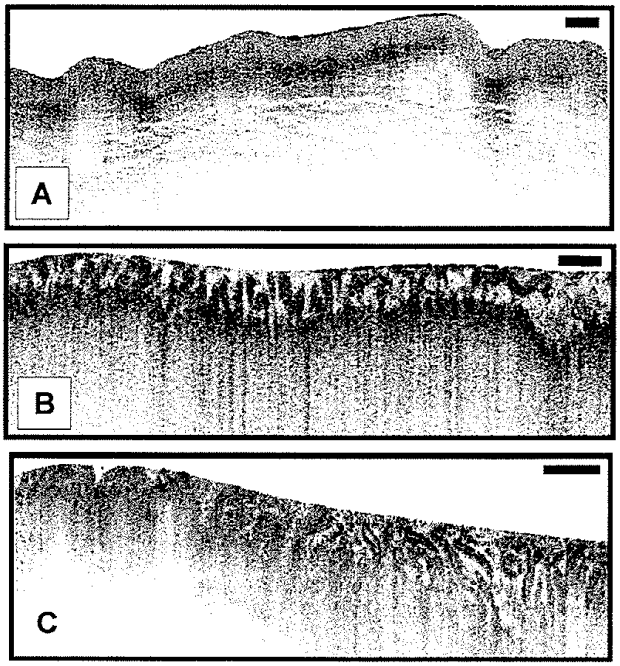

Fig. 6 In vitro OCT images of human gastrointestinal tissues and pathology. A) normal human esophagus showing squamous epithelial structure, B) normal colon with crypt structures, and C) ampullary carcinoma showing associated disruption of normal epithelial organization. The carcinoma is on the left of the image. These images illustrate the ability of OCT to discriminate architectural morphology relevant to the detection of early neoplastic changes. From reference [12].

of normal esophagus, normal colon, and ampullary carcinoma. The OCT image of the esophagus shows normal morphology of the mucosa and submucosa. The upper portion of the mucosa appears homogenous in the OCT image and is associated with squamous epithelial architecture. The muscularis mucosa is more highly reflective than the mucosa and a gap can be seen between the muscularis mucosa and the submucosa. The OCT image of the colon shows normal glandular organization associated with collumnar epithelial structure. The mucosa and muscularis mucosa can be differentiated due to the different backscattering characteristics within each layer. Architectural morphology such as crypts or glands within the mucosa can also be seen. Finally, the OCT image of ampullary carcinoma shows disruption of architectural morphology or glandular organization. The area on the right of the image is normal, while the carcinoma is on the left of the image. The crypt structures are dilated and distorted in the middle of the image with complete loss of structure in the carcinoma.

Endoscopic ultrasound has recently been introduced as a new technology for high resolution endoscopic imaging [71-77]. Using ultrasound frequencies in the range of 10-30 MHz, axial resolutions in the range of 100 μm can be achieved [78-80]. Imaging of the esophagus or bowel requires filling the lumen with saline or using a liquid filled balloon to couple the ultrasound into the tissue. .Ultrasound can be used as an adjunct to endoscopy to diagnose and stage early esophageal and gastric neoplasms. Impressive results have been achieved using high frequency endoscopic ultrasound which demonstrate the differentiation of mucosal and submucosal structures.

Using OCT image resolutions of 15 um or higher can be achieved. This resolution enables the visualization of tissue architectural morphology. Changes in architectural morphology such as these can be used for the screening and the diagnosis of early neoplastic changes. The imaging depth of OCT is 2-3 mm, less than that of ultrasound. However, for diseases that originate from or involve the mucosa, submucosa, and muscular layers, imaging the microscopic structure of small lesions is well within the range of OCT. Conventional excisional biopsy often suffers from high false negative rates because the biopsy process relies on sampling tissue and the diseased tissues can easily be missed. OCT could be used to identify suspect lesions and to guide excisional biopsy in order and reduce the false negative rates. This would reduce the number of costly biopsies and at the same time clinical diagnosis could be made using biopsy and histopathology, which is a well established standard. In the future, after more extensive clinical data are available, it may be possible to use OCT directly for the diagnosis or staging of certain types of neoplasias. For example OCT might be used to assess the presence of submucosal versus mucosal involvement in early gastric cancer.

Guiding surgical intervention

Another large class of applications for OCT is guiding surgical intervention. The ability to see beneath the surface of tissue in real time can guide surgery near sensitive structures such as

vessels or nerves and assist in microsurgical procedures [15,17]. Optical instruments such as surgical microscopes are routinely used to magnify tissue to prevent iatrogenic injury and to guide delicate surgical techniques. OCT can be easily integrated with surgical microscopes. Hand held OCT surgical probes and laparoscopes have also been demonstrated [26].

One example of a surgical application for OCT is the repair of small vessels and nerves following traumatic injury. A technique capable of real time, subsurface, three-dimensional, micron-scale imaging would permit the intraoperative monitoring of microsurgical procedures, giving immediate feedback to the surgeon which could enable difficult procedures and improve outcome. To demonstrate the use of OCT imaging for diagnostically assessing microsurgical procedures in vitro studies were performed using a OCT microscope [17].

Figure 7 shows in vitro OCT images of an arterial anastomosis of a rabbit inguinal artery demonstrating the ability of OCT to assess internal structure and luminal patency. An artery segment was bisected cross-sectionally with a scalpel and then re-anastomosed using a No. 10-0 nylon suture with a 50 μm diameter needle in a continuous suture. For precise registration of 3D

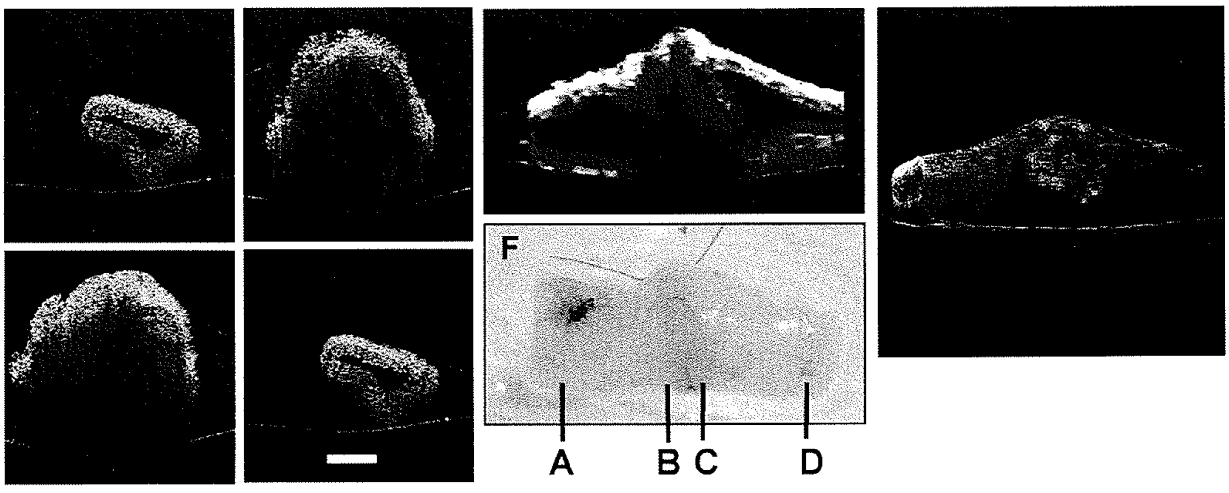

Fig. 7 OCT images of an anastomosis in a rabbit artery. The 1 mm diameter rabbit artery was anastomosed with a continuous suture as seen in en face image (F). The lines in F indicate the OCT imaging planes. A,D) Opposite ends of the anastomosis showing multi-layered structure of the artery with a patent lumen. B) Partially obstructed lumen and the presence of a thrombogenic flap. C) Fully obstructed portion of the anastomosis site. G,H) Three-dimensional projections which can be arbitrary sectioned at any plane. From reference [17].

images, the anastomosed specimen was positioned on a micron step size, computer-controlled, motorized translation stage in the OCT microscope. A series of 40 cross-sectional images were acquired perpendicular to the long axis at 100 μm spacing. The specimen was also digitally imaged with a CCD camera. Cross-sectional OCT images (2.2 x 2.2 mm, 250 x 600 pixel) and 3-D projections of a 1 mm diameter rabbit inguinal artery are shown. Figures 7A through 7D show transverse images at different positions through the anastomosis. The images of the ends of the artery clearly show arterial morphology corresponding to the intimal, medial, and adventitial layers of the elastic artery. The image from the site of the anastomosis shows that the lumen was obstructed by a tissue flap. By assembling a series of cross-sectional 2-D images, a 3-D dataset was produced. Arbitrary planes can be selected and corresponding sections displayed. Three-dimensional projections of the arterial anastomosis are shown in Figure 7. The three dimensional views can show microstructural features which are not evident in single cross sectional images.

Optical coherence tomography can provide high-resolution, real time, cross-sectional imaging subsurface structures. This capability could be used to guide surgery near sensitive structures such as vessels and nerves. Imaging can be performed using simple hand held instruments. OCT could be integrated with the surgical intervention in order to provide real time feedback. Preliminary studies have been performed to investigate combining OCT imaging with laser ablation [81]. Finally, three dimensional OCT imaging can be performed using a microscope platform. Rendering and reconstruction algorithms can be applied to produce a three dimensional representation to assess the spatial orientation of morphology.

Catheter and endoscopic OCT imaging

Because OCT imaging technology is fiber optic based, it can be easily integrated with many standard medical diagnostic instruments to enable internal body imaging. OCT laparascopes and hand held surgical probes have recently been demonstrated [26]. Using fiber

optics, a small diameter transverse scanning catheter/endoscope has been developed and demonstrated for in vivo imaging in animals [31]. Figure 8 shows a schematic of the OCT catheter/endoscope. The catheter/endoscope consists of a single mode optical fiber encased in a hollow rotating torque cable. At the distal end of the catheter, the fiber is coupled to a graded index GRIN lens and a microprism to direct the OCT beam radially, perpendicular to the axis of the catheter [24]. The rotating cable and distal optics are encased in a transparent housing. The OCT beam is scanned by rotating the cable to permit cross sectional transluminal imaging, in a radar-like pattern, in vessels or hollow organs. Figure 9 shows a photograph of the prototype catheter. The catheter/endoscope has a diameter of 2.9 French or 1 mm, comparable to the size of a standard intravascular ultrasound catheter. This is small enough to allow imaging in a human coronary artery or insertion through the accessory port of a standard endoscope or bronchoscope.

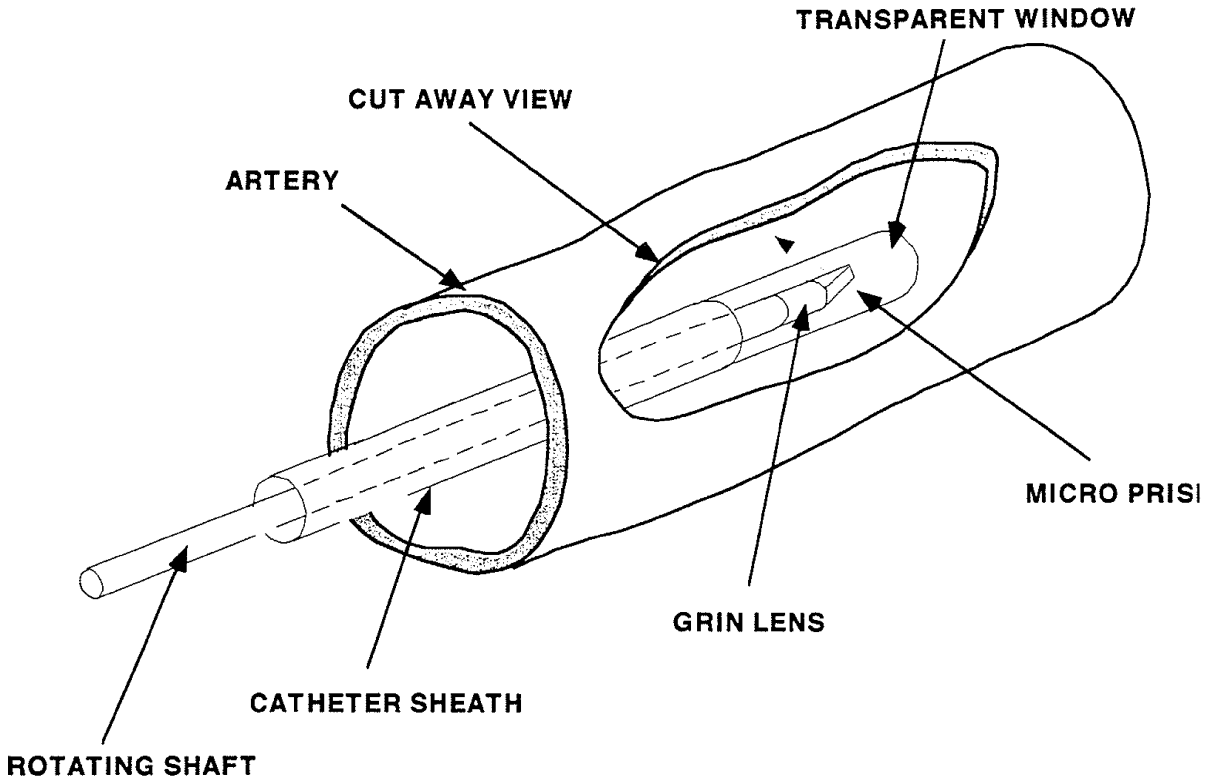

Fig. 8 Schematic of OCT catheter for transverse, intraluminal imaging. A single-mode fiber is contained within a rotating flexible speedometer cable which is enclosed in a protective plastic sheath. The distal end focuses the OCT beam at 90 degree from the catheter axis. From reference [24].

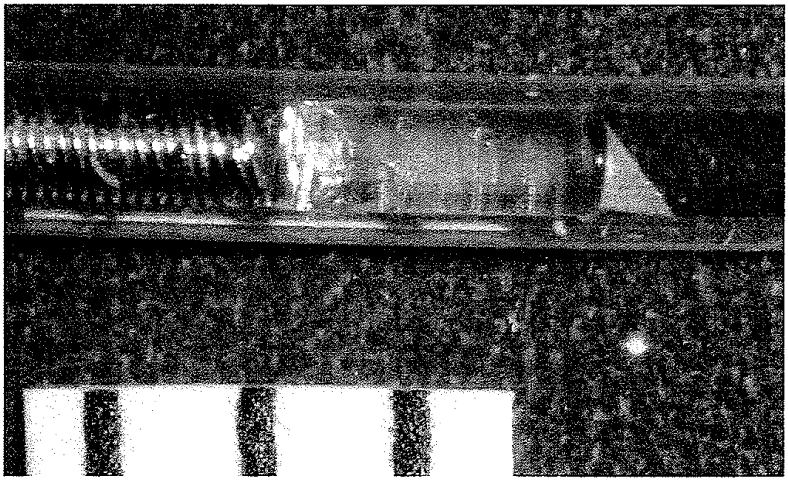

Fig. 9 Photograph of prototype OCT catheter for transverse, intraluminal imaging. The diameter of the catheter is 2.9 F or 1 mm.

The catheter-endoscope OCT system enables the acquisition of in vivo images of internal organ systems. In vivo imaging of the pulmonary, gastrointestinal, and urinary tracts as well as arterial imaging have been demonstrated in New Zealand White rabbits [31]. A short pulse Cr^{4+}:forsterite laser was used as the light source for OCT system to achieve high resolution with real time image acquisition rates [29]. The laser output wavelength was centered near 1280 nm with a FWHM spectral bandwidth of 75 nm and 5-10 mW power was incident on the tissue. This yields an axial resolution of 10 μm and a signal to noise ratio of 110 decibels (dB). In order to achieve high-speed imaging at several frames per second, a novel high speed scanning optical delay line was used in the OCT interferometer [39].

Figure 10 shows an example of in vivo OCT catheter/endoscope imaging of the rabbit gastrointestinal tract. Imaging could be performed with either 256 or 512 lateral pixels, corresponding to image acquisition times of 125 ms or 250 ms, respectively. The image shown was obtained with a 512 pixel lateral resolution at 4 frames per second in order to optimize lateral sampling. The two-dimensional image data were displayed using a polar coordinate transformation and inverse gray scale. Data were recorded in both Super VHS and digital format. As shown in Figure 10, OCT images of the in vivo esophagus permitted differentiation of the

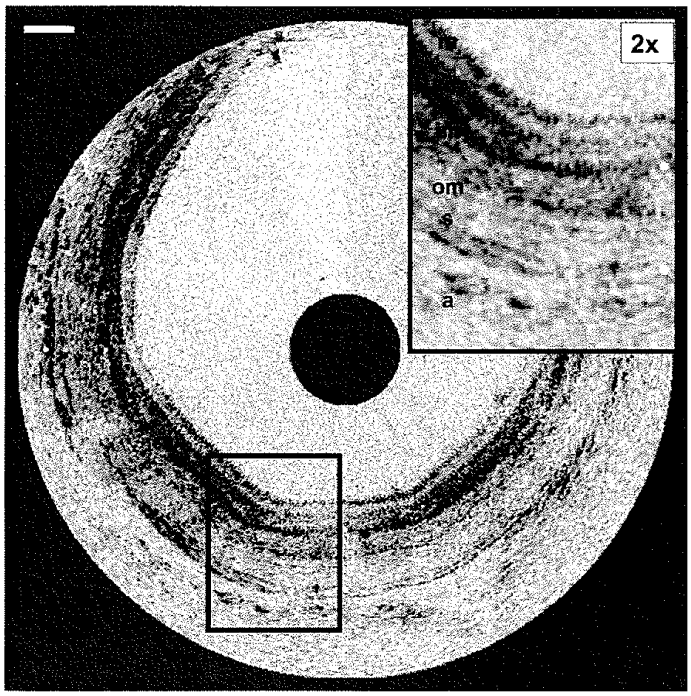

Fig. 10 OCT catheter/endoscope image in vivo of the esophagus of a New Zealand White Rabbit. The image clearly differentiates the layers of the esophagus including the mucosa, submucosa, inner muscularis, and outer muscularis. From reference [31].

layers of the esophageal wall. The mucosa was readily identifiable because of its low optical backscattering compared with the submucosa. The ability to differentiate mucusal versus submucosal invasion of early cancers can be an important criteria for determining therapy in early cancers.

These studies demonstrate the feasibility of performing OCT imaging of internal organ systems and suggest a range of future clinical applications. Preliminary OCT imaging studies in patients have been reported [32,70]. More systematic OCT imaging studies comparing imaging with histological or other diagnostic endpoints are needed. Other research groups as well as our group are currently performing OCT imaging studies in patients and we expect results to be published shortly.

Cellular level OCT imaging

The development of high resolution OCT is also an important area of active research.

Increasing resolutions to the cellular and subcellular level are important for many applications including the diagnosis of early neoplasias. As discussed previously, the axial resolution of OCT is determined by the coherence length of the light source used for imaging. Light sources for OCT imaging should have a short coherence length or broad bandwidth, but also must have a single spatial mode so that they can be used in conjunction with interferometry. In addition, since the signal to noise depends on the incident power, light sources with average powers of several milliwatts are typically necessary to achieve real time imaging. One approach for achieving high resolution is to use short pulse femtosecond solid state lasers as light sources [28,29].

High resolution OCT imaging has been demonstrated in vivo in developmental biology specimens [30]. Figure 11 show an example of high resolution OCT images of a *Xenopus laevis* (African frog) tadpole. A short pulse Cr^{4+}:Forsterite laser which operates near 1300 nm was used as the light source for these measurements. The free space axial resolution was 5.1 μm. Assuming an average index of 1.35 for these specimens, the *in vivo* axial resolution was ~ 3.8 μm. The transverse resolution was determined by the focussed spot size of the beam. For these studies the focussed spot was 9 μm diameter, resulting in a 100 μm confocal parameter or depth of field.

Figure 11 shows a comparison between OCT images and corresponding histology. Figures 11A/B show the presence of multiple nuclei and cell membranes. The seemingly wide cell membranes in the OCT images are actually composed of membranes and extracellular matrix. The OCT image in Figure 11A shows cells with varying size and nuclear-to-cytoplasmic ratios. An enlarged OCT image of a dividing cell is shown in Figure 11C with corresponding histology in Figure 11D. Two distinct nuclei are clearly shown and pinching of the cell membrane is also visible.

In developmental biology, the ability to image cellular and subcellular structure can be used to study mitotic activity and cell migration which occur during development. The extension

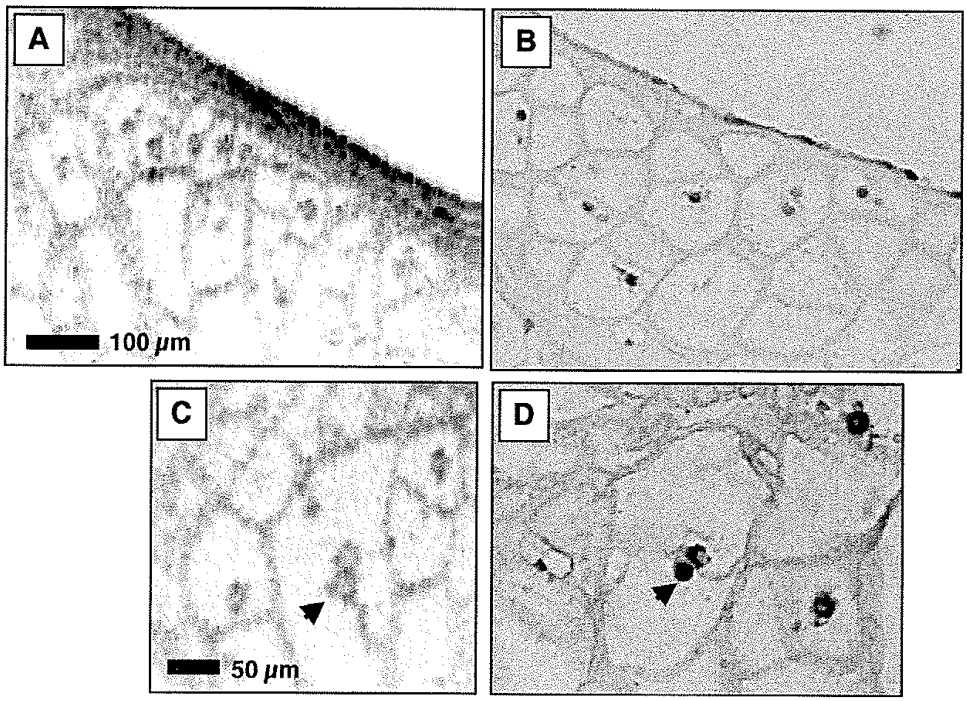

Fig. 11 High resolution OCT images of a Xenopus laevis (African Frog) tadpole in vivo. Figures A/B shows OCT and histology of mesenchymal cells of differing sizes. Cell membranes and individual cell nuclei are visible. Exact matches with histology are difficult to achieve at these dimensions. C/D Enlarged image of dividing cell correlates well with histology. From reference [30].

of these results to human cells has important implications, however, since differentiated human cells are smaller than developing cells, additional improvements in resolution are necessary to achieve this objective. In ophthalmology, improving resolution should allow more precise morphmetric measurements of retinal features such as retinal thickness and retinal nerve fiber layer thickness which are relevant for the detection and screening for macular edema and glaucoma. High resolution imaging would also improve OCT diagnosis of early neoplastic changes. Standard OCT image resolutions are sufficient to image architectural morphology on the 10-15 um scale and can identify many early neoplastic changes. The ability to image with cellular level resolution would not only enhance the spectrum of early neoplasias and dysplasia that could be imaged, but also improve sensitivity and specificity.

Summary

OCT can perform a type of optical biopsy, the micron scale imaging of tissue morphology in situ and in real time. Image information is available immediately without the need for excision and histological processing of a specimen. The development of high resolution and high speed OCT technology as well as OCT compatible catheter-endoscopes and other delivery system represent enabling steps for many future OCT imaging clinical applications. More research remains to be done and numerous clinical studies must be performed in order to determine in which clinical situations OCT can play a role. However, the unique capabilities of OCT imaging suggest that it has the potential to have a significant impact on the diagnosis and clinical management of many diseases.

Acknowledgements

This manuscript is a summary of a plenary lecture presented at the 19th Congress of the Japan Laser Surgery and Medicine Society, which was held on September 24 and 25, 1998 in Tokyo, Japan. The author gratefully acknowledges the support of the Fujinon Corporation which made participation in this conference possible. The scientific contributions of Drs. Xingde Li, Wolfgang Drexler, Joel Schuman, Carmen Puliafito, Michael Hee, Brett Bouma, Gary Tearney, and Juergen Herrmann are gratefully acknowledged. This research is supported in part by the National Institutes of Health, Contracts NIH-9-RO1-CA75289-01, NIH-9-RO1-EY11289-13, NIH-RO1-AR44812-02, NIH-1-R29-HL55686-01A1, the Office of Naval Research Medical Free Electron Laser Program, Contract N000014-97-1-1066, and the Whittaker Foundation Contract 96-0205. Dr. Boppart was supported by the Air Force Palace Knight program.

References

1. Huang D, Swanson EA, Lin CP, Schuman JS, Stinson WG, Chang W, Hee MR, Flotte T, Gregory K, Puliafito CA, Fujimoto JG. Optical coherence tomography. Science

1991;254:1178-80.

2. Swanson EA, Izatt JA, Hee HR, Huang D, Fujimoto JG, Lin CP, Schuman JS, Puliafito CA. In vivo retinal imaging using optical coherence tomography. Opt Lett 1993;18:1864-66.
3. Fercher AF, Hitzenberger CK, Drexler W, Kamp G, Sattmann H. In vivo optical coherence tomography. Am J Ophthalmol 1993;116:113-14.
4. Hee MR, Izatt JA, Swanson EA, Huang D, Lin CP, Schuman JS, Puliafito CA, Fujimoto JG. Optical coherence tomography of the human retina. Arch Ophthalmol 113;1995:325-32.
5. Puliafito CA, Hee MR, Lin CP, Reichel E, Schuman JS, Duker JS, Izatt JA, Swanson EA, Fujimoto JG. Imaging of macular disease with optical coherence tomography (OCT). Ophthalmology 1995;102:217-29.
6. Puliafito CA, Hee MR, Schuman JS, Fujimoto JG. Optical coherence tomography of ocular diseases. Thorofare N.J: Slack, Inc, 1995).
7. Schmitt JM, Yadlowsky MJ, Bonner RF. Subsurface imaging of living skin with optical coherence microscopy. Dermatology 1995;191:93-98.
8. Brezinski ME, Tearney GJ, Bouma BE, Izatt JA, Hee MR, Swanson EA, Southern JF, Fujimoto JG. Optical coherence tomography for optical biopsy: properties and demonstration of vascular pathology. Circulation 1996;93:1206-13.
9. Fujimoto JG, Brezinski ME, Tearney GJ, Boppart SA, Bouma BE, Hee MR, Southern JF, Swanson EA. Biomedical imaging and optical biopsy using optical coherence tomography. Nat Med 1995;1:970-72.
10. Brezinski ME, Tearney GJ, Weissman NJ, Boppart SA, Bouma BE, Hee MR, Weyman AE, Swanson EA, Southern JF, Fujimoto JG. Assessing atherosclerotic plaque morphology: comparison of optical coherence tomography and high frequency intravascular ultrasound. Brit Heart J 1997;77:397-404.
11. Izatt JA, Kulkarni MD, Wang HW, Kobayashi K, Sivak MV. Optical coherence tomography and microscopy of gastrointestinal tissues. IEEE J Sel Topics Quantum Electron 1996;2:1017-28.
12. Tearney GJ, Brezinski ME, Southern JF, Bouma BE, Boppart SA, and Fujimoto JG. Optical biopsy in human gastrointestinal tissue using optical coherence tomography. Am J Gastroenterology 1997;92:1800-04.
13. Tearney GJ, Brezinski ME, Southern JF, Bouma BE, Boppart SA, Fujimoto JG. Optical biopsy in human pancreatobiliary tissue using optical coherence tomography. Dig Dis Sci 43;1998:1193-99.
14. Tearney GJ, Brezinski ME, Southern JF, Bouma BE, Boppart SA, Fujimoto JG. Optical

biopsy in human urologic tissue using optical coherence tomography. J Urology 1997;157:1915-19.

15. Brezinski ME, Tearney GJ, Boppart SA, Swanson EA, Southern JF, Fujimoto JG. Optical biopsy with optical coherence tomography, feasibility for surgical diagnostics. J Surg Res 1997;71:32-40.
16. Herrmann JM, Brezinski ME, Bouma BE, Boppart SA, Pitris C, Fujimoto JG. Two and three dimensional high resolution imaging of the human oviduct with optical coherence tomography. Fertility Sterility 1998;70:155-58.
17. Boppart SA, Bouma BE, Pitris C, Tearney GJ, Southern JF, Brezinski ME, Fujimoto JG. Intraoperative assessment of microsurgery with three-dimensional optical coherence tomography. Radiology 1998;208:81-86.
18. Roper SN, Moores MD, Gelikonov GV, Feldchstein FI, Beach NM, King MA, Gelinkonov VM, Sergeev AM, Reitze DH. In vivo detection of experimentally induced cortical dysgenesis in the adult rat neocortex using optical coherence tomography. J Neuroscience Meth 1998;80:91-98.
19. Pitris C, Goodman A, Boppart SA, Libus JJ, Fujimoto JG, Brezinski ME. High resolution imaging of gynecological neoplasms using optical coherence tomography. Obstet Gynocol 1999;93:135-39.
20. Herrmann JM, Pitris C, Bouma BE, Boppart SA, Fujimoto JG, Brezinski ME. High resolution imaging of normal and osteoartheritic cartilage with optical coherence tomography. J Rheumatology 1999;26:627-35.
21. Boppart SA, Brezinski ME, Bouma B, Tearney GJ, Fujimoto JG. Investigation of developing embryonic morphology using optical coherence tomography. Dev Biology 1996;177:54-63.
22. Boppart SA, Brezinski ME, Tearney GJ, Bouma BE, Fujimoto JG. Imaging developing neural morphology using optical coherence tomography. J Neuroscience Meth 1996;2112:65-72.
23. Boppart SA, Tearney GJ, Bouma BE, Southern JF, Brezinski ME, Fujimoto JG. Noninvasive assessment of the developing xenopus cardiovascular system using optical coherence tomography. Proc Nat Academy Sci 1997;94:4256-61.
24. Tearney GJ, Boppart SA, Bouma BE, Brezinski ME, Weissman NJ, Southern JF, Fujimoto JG. Scanning single mode catheter/endoscope for optical coherence tomography. Opt Lett 1996;21:543-45.
25. Tearney GJ, Brezinski ME, Boppart SA, Bouma BE, Weissman N, Southern JF, Swanson EA, Fujimoto JG. Catheter-based optical imaging of a human coronary artery. Circulation 1996;94:3013.

26. Boppart SA, Bouma BE, Pitris C, Tearney GJ, Fujimoto JG, Brezinski ME. Forward-imaging instruments for optical coherence tomography. Opt Lett 1997;22:1618-20.
27. Tearney GJ, Bouma BE, Boppart SA, Golubovic B, Swanson EA, Fujimoto JG. Rapid acquisition of in vivo biological images using optical coherence tomography. Opt Lett 1996;21:1408-10.
28. Bouma B, Tearney GJ, Boppart SA, Hee MR, Brezinski ME, Fujimoto JG. High resolution optical coherence tomographic imaging using a modelocked Ti:Al_2O_3 laser source. Opt Lett 1995;20:1-3.
29. Bouma BE, Tearney GJ, Bilinsky IP, Golubovic B, Fujimoto JG. Self-phase-modulated Kerr-lens mode-locked Cr:forsterite laser source for optical coherence tomography. Opt Lett 1996;21:1839-42.
30. Boppart SA, Bouma BE, Pitris C, Southern JF, Brezinski ME, Fujimoto JG. In vivo cellular optical coherence tomography imaging. Nat Med 1998;4:861-65.
31. Tearney GJ, Brezinski ME, Bouma BE, Boppart SA, Pitris C, Southern JF, Fujimoto JG. In vivo endoscopic optical biopsy with optical coherence tomography. Science 1997;276:2037-39.
32. Sergeev AM, Gelikonov VM, Gelikonov GV, Feldchtein FI, Kuranov RV, Gladkova ND, Shakhova NM, Snopova LB, Shakov AV, Kuznetzova IA, Denisenko AN, Pochinko VV, Chumakov YP, Streltzova OS. In vivo endoscopic OCT imaging of precancer and cancer states of human mucosa. Opt Express 1997;1:432-40.
33. Takada K, Yokohama I, Chida K, Noda J. New measurement system for fault location in optical waveguide devices based on an interferometric technique. Appl Opt 1987;26:1603-08.
34. Youngquist RC, Carr S, Davies DEN. Optical coherence domain reflectometry: A new optical evaluation technique. Opt Lett 1987;12:158-60.
35. Fercher AF, Mengedoht K, Werner W. Eye-length measurement by interferometry with partially coherent light. Opt Lett 1988;13:186-88.
36. Hitzenberger CK. Measurement of the axial eye length by laser Doppler interferometry. Invest Ophthalmol Vis Sci 1991;32:616-24.
37. Huang D, Wang J, Lin CP, Puliafito CA, Fujimoto JG. Micron-resolution ranging of cornea and anterior chamber by optical reflectometry. Lasers Surg Med 1991;11:419-425.
38. Morgner U, Kaertner FX, Cho SH, Chen Y, Haus HA, Fujimoto JG, Ippen EP, Scheuer V, Angelow G, Tschudi T. Sub two-cycle fs pulses from a Kerr-lens mode-locked Ti:sapphire laser. Opt Lett 1999;24:411-13.
39. Tearney GJ, Bouma BE, Fujimoto JG. High-speed phase- and group-delay scanning with a grating-based phase control delay line. Opt Lett 1997;22:1811-13.

40. Weiner AM, Heritage JP, Kirschner EM. High resolution femtosecond pulse shaping. J Opt Soc Am B 1986;5:1563-72.
41. Thurston RN, Heritage JP, Weiner AM, Tomlison WJ. Analysis of picosecond pulse shape synthesis by spectral masking in a grating pulse compressor. IEEE J Quantum Elect 1986;QE-22:682-96.
42. Izatt JA, Hee MR, Swanson EA, Lin CP, Huang D, Schuman JS, Puliafito CA, Fujimoto JG. Micrometer-scale resolution imaging of the anterior eye in vivo with optical coherence tomography. Arch Ophthalmol 1994;112:1584-89.
43. Hee MR, Puliafito CA, Wong C, Duker JS, Rutledge B, Schuman JS, Swanson EA, Fujimoto JG. Quantitative assessment of macular edema with optical coherence tomography. Arch Ophthalmol 1995;113:1019-29.
44. Hee MR, Puliafito CA, Duker JS, Reichel E, Coker JG, Wilkins JR, Schuman JS, Swanson EA, Fujimoto JG. Topography of diabetic macular edema with optical coherence tomography. Ophthalmology 1998;105:360-70.
45. Schuman JS, Hee MR, Puliafito CA, Wong C, Pedut-Kloizman T, Lin CP, Hertzmark E, Izatt JA, Swanson EA, Fujimoto JG. Quantification of nerve fiber layer thickness in normal and glaucomatous eyes using optical coherence tomography. Arch Ophthalmol 1995;113:586-96.
46. Schuman JS, Pedut-Kloizman T, Hertzmark E, Hee MR, Wilkins JR, Coker JG, Puliafito CA, Fujimoto JG, Swanson EA. Reproducibility of nerve fiber layer thickness measurements using optical coherence tomography. Ophthalmol 1996;103:1889-98.
47. Hee MR, Puliafito CA, Wong C, Duker JS, Reichel E, Schuman JS, Swanson EA, Fujimoto JG. Optical coherence tomography of macular holes. Ophthalmol 1995;102:748-56.
48. Hee MR, Puliafito CA, Wong C, Reichel E, Duker JS, Schuman JS, Swanson EA, Fujimoto JG. Optical coherence tomography of central serous chorioretinopathy. Am J Ophthalmol 1995;120:65-74.
49. Hee MR, Baumal CR, Puliafito CA, Duker JS, Reichel E, Wilkins JR, Coker JG, Schuman JS, Swanson EA, Fujimoto JG. Optical coherence tomography of age-related macular degeneration and choroidal neovascularization. Ophthalmol 1996;103:1260-70.
50. Wilkins JR, Puliafito CA, Hee MR, Duker JS, Reichel E, Coker JG, Schuman JS, Swanson EA, Fujimoto JG. Characterization of epiretinal membranes using optical coherence tomography. Ophthalmol 1996;103:2142-51.
51. Krivoy D, Gentile R, Liebmann JM, Stegman Z, Walsh JB, Ritch R. Imaging congenital optic disc pits and associated maculopathy using optical coherence tomography. Arch Ophthalmol 1996;114:165-70.
52. Schaudig U, Hassenstein A, Bernd A, Walter A, Richard G. Limitations of imaging choroidal

tumors in vivo by optical coherence tomography. Graefe's Arch Clin Exp Ophthalmol 1998;236:588-592.

53. Lincoff H, Kreissig I. Optical coherence tomography of pneumatic displacement of optic disc pit aculopathy. Br J Ophthalmol 1998;82:367-72.
54. Toth CA, Birngruber R, Boppart SA, Hee MR, Fujimoto JG, DiCarlo CD, Swanson EA, Cain CP, Narayan DG, Noojin GD, Roach WP. Argon laser retinal lesions evaluated in vivo by optical coherence tomography. Am J Ophthalmol 1997;123:188-98.
55. Toth CA, Narayan DG, Boppart SA, Hee MR, Fujimoto JG, Birngruber R, Cain CP, Di Carlo CD, Roach WP. A comparison of retinal morphology viewed by optical coherence tomography and by light microscopy. Arch Ophthalmol 1997;115:1425-28. Published erratum appears in Arch Ophthalmol 1998;116:77.
56. Parsa P, Jacques S, Nishioka N. Optical properties of rat liver between 350 and 2200 nm. Appl Opt 1989;28:2325-30.
57. Schmitt JM, Knuttel A, Yadlowsky M, Eckhaus AA. Optical coherence tomography of a dense tissue: statistics of attenuation and backscattering. Phys Med Biol 1994;39:1705.
58. Falk E. Plaque rupture with severe pre-existing stenosis precipitating coronary thrombosis, characteristics of coronary atherosclerotic plaques underlying fatal occlusive thrombi. Br Heart J 1983;50:127-34.
59. Davies MJ, Thomas AC. Plaque fissuring- the cause of acute myocardial infarction, sudden ischemic death, and crescendo angina. Br Heart J 1983;53:363-73.
60. Richardson PD, Davies MJ, Born GVR. Influence of plaque configuration and stress distribution on fissuring of coronary atherosclerotic plaques. Lancet 1989;i:941-944.
61. Fuster VL, Badimon L, Badimon JJ, et al. The pathogenesis of coronary artery disease and the acute coronary syndromes. New Eng J Med 1992;326:242-49.
62. Loree HM, Lee R. Stress analysis of unstable plaque Circ Res 1992;71:850.
63. Gillum RF. Sudden coronary death in the United States; 1980-1985. Circulation 1989;79:756-64.
64. Nissen SE, Gurley JC, Booth DC, DeMaria AN. Intravascular ultrasound of the coronary arteries: current applications and future directions. Am J Card 1992;69:18H-29H.
65. Lee D-Y, Eigler N, Luo H, Steffen W, Tabak S, Seigel RJ. Intravascular coronary ultrasound imaging, is it useful? J Am Coll Card 1994;Suppl. 241A.
66. Benkeser PJ, Churchwell AL, Lee C, Aboucinaser DM. Resolution limitations in intravascular ultrasound imaging. J Am Soc Echocard 1993;6:158-65.
67. Fujimoto JG, Boppart SA, Tearney GJ, Bouma BE, Pitris C, Brezinski ME. High resolution in vivo intraarterial imaging with optical coherence tomography. Heart (in press).

68. Kobayashi K, Izatt JA, Kulkarni MD, Willis J, Sivak MV, Jr. High-resolution cross-sectional imaging of the gastrointestinal tract using optical coherence tomography: Preliminary results. Gastrointest Endosc 1998;47:515-23.
69. Boppart SA, Goodman A, Libus, Pitris C, Jesser C, Brezinski ME, Fujimoto JG. High resolution imaging of endometriosis and ovarian carcinoma with optical coherence tomography: Feasibility for laparoscopic-based imaging. Br J Obstetrics, (in press).
70. Feldchtein FI, Gelikonov GV, Gelikonov VM, Kuranov RV, Sergeev AM, Gladkova ND, Shakhov AV, Shakhova NM, Snopova LB, Terent'eva AB, Zagainova EV, Chumakov YP, Kuznetzova IA. Endoscopic applications of optical coherence tomography. Opt Express 1998;3:257.
71. Kimmey MB, Martin RW, Haggitt RC, et al. Histologic correlates of gastrointestinal ultrasound images. Gastroenterology 1989; 96:433-441.
72. Botet JF, Lightdale C. Endoscopic ultrasonography of the upper gastrointestinal tract. Radiologic Clinics of North America 1992;30:1067-83.
73. Hawes RH. New staging techniques: Endoscopic Ultrasound. Cancer 1993;71:4207-13.
74. Furukawa T, Naitoh Y, Tsukamoto Y. New technique using intraductal ultrasound for diagnosis of diseases of the pancreatobiliary system. J Ultrasound Med 1992;11:607-12.
75. Rosh T. Endoscopic ultrasonography. Endoscopy 1994;26:148-68.
76. Falk GW, Catalano MF, Sivak MV Jr, Rice TW, Van Dam J. Endosonography in the evaluation of patients with Barrett's esophagus and high grade dysplasia. Gastrointest Endosc 1994;40:207-12.
77. Hizawa K, Suekane H, Aoyagi K, Matsumoto T, Nakamura S, Fujishima M. Use of endosonographic evaluation of colorectal tumor depth in determining the appropriatness of endoscopic mucosal resection. Am J Gastroenterol 1996;91:768-71.
78. Wiersema MJ, Wiersema LM. High-resolution 25-MHz ultrasonography of the gastrointestinal wall: histologic correlates. Gastrointestinal Endoscopy 1993;39:499-504.
79. Yanai H, Tada M, Karita M, Okita K. Diagnostic utility of 20-megahertz linear endoscopic ultrasonography in early gastric cancer. Gastrointest Endosc 1996;44:29-33.
80. Yanai H, Yoshida T, Harada T, Matsumoto Y, Nishiaki M, Shigemitsu T, et al. Endoscopic ultrasonography of superficial esophageal cancers using a thin ultrasound probe system equipped with switchable radial and linear scanning modes. Gastrointest Endosc 1996;44:578-82.
81. Boppart SA, Herrmann J, Pitris C, Stamper DL, Brezinski ME, Fujimoto JG. High-resolution optical coherence tomography guided laser ablation of surgical tissue. J Surgical Res, in press.